Accepted for publication in *The Astrophysical Journal Letters*
Preprint typeset using LaTeX style emulateapj v. 10/09/06



# LEO V: SPECTROSCOPY OF A DISTANT AND DISTURBED SATELLITE*

M.G. Walker[1], V. Belokurov[1], N.W. Evans[1], M.J. Irwin[1], M. Mateo[2], E.W. Olszewski[3], G. Gilmore[1]

*Draft version February 17, 2009*

## ABSTRACT

We present a spectroscopic study of Leo V, a recently discovered satellite of the Milky Way (MW). From stellar spectra obtained with the MMT/Hectochelle spectrograph we identify seven likely members of Leo V. Five cluster near the Leo V center ($R < 3'$) and have velocity dispersion $2.4^{+2.4}_{-1.4}$ km s$^{-1}$. The other two likely members lie near each other but far from the center ($R \sim 13' \sim 700$ pc) and inflate the global velocity dispersion to $3.7^{+2.3}_{-1.4}$ km s$^{-1}$. Assuming the five central members are bound, we obtain a dynamical mass of $M = 3.3^{+9.1}_{-2.5} \times 10^5 M_\odot$ ($M/L_V = 75^{+230}_{-58}[M/L_V]_\odot$). From the stacked spectrum of the five central members we estimate a mean metallicity of [Fe/H]$= -2.0 \pm 0.2$ dex. Thus with respect to dwarf spheroidals of similar luminosity, Leo V is slightly less massive and slightly more metal-rich. Since we resolve the central velocity dispersion only marginally, we do not rule out the possibility that Leo V is a diffuse star cluster devoid of dark matter. The wide separation of its two outer members implies Leo V is losing mass; however, its large distance ($D \sim 180$ kpc) is difficult to reconcile with MW tidal stripping unless the orbit is very radial.

*Subject headings:* galaxies: dwarf — galaxies: kinematics and dynamics — (galaxies:) Local Group — (cosmology:) dark matter —

## 1. INTRODUCTION

The recent discoveries of thirteen ultra-faint Milky Way (MW) satellites (e.g., Willman et al. 2005; Zucker et al. 2006; Belokurov et al. 2007) have reshaped the census of Local Group galaxies and increased our ability to test cosmological models using objects available in our own neighborhood. The new satellites, discovered primarily with data from the Sloan Digital Sky Survey (SDSS; York et al. 2000), extend the galaxy luminosity function by three orders of magnitude, to $\sim 10^3 L_\odot$ (Koposov et al. 2008). Spectroscopic surveys (e.g., Martin et al. 2007, Simon & Geha 2007, SG07 hereafter) of their few red giants reveal that these systems extend scaling relationships according to which the least luminous dwarf galaxies are the most dominated by dark matter and most metal-poor (e.g., Mateo 1998; Kirby et al. 2008).

Leo V, the most recent addition to the ensemble of MW satellites, was originally detected as a modest ($\sim 4\sigma$) overdensity of stars in SDSS data (Belokurov et al. 2008, "Paper I" hereafter). Slightly deeper photometry from the Isaac Newton Telescope (INT) reveals a blue horizontal branch (BHB) and red clump in addition to the red giant branch (RGB; Figure 3 of Paper I). The apparent magnitude of its BHB implies Leo V has $M_V \sim -4.3$ and lies at a distance of $\sim 180$ kpc, placing it at a (deprojected) distance of just $\sim 20$ kpc from another SDSS dSph, Leo IV (Belokurov et al. 2007). As the systemic line-of-sight velocities of Leos IV and V differ by just $\sim 40$ km s$^{-1}$, the two objects may represent the smallest companions among the known MW satellites.

With this letter we present an initial spectroscopic study of individual stars in Leo V. Despite heavy contamination by the Galactic foreground, we are able to identify seven likely members of Leo V. We use the stacked spectrum of these members to estimate Leo V's mean metallicity, and we use their spatial and velocity distributions to investigate Leo V's dynamical state and plausible dark matter content.

## 2. OBSERVATIONS, DATA & MEMBERSHIP

On 2008 May 28 and 30 we obtained medium-resolution spectra of 158 Leo V targets using the Hectochelle spectrograph at the MMT Observatory. We maximized the chance of observing Leo V members by choosing targets based on proximity to the center of Leo V and to the locus of its RGB (Figure 3 of Paper I). We extracted and calibrated spectra following the procedure described in detail by Mateo et al. (2008). The Hectochelle spectra span the wavelength range $5150 - 5300$ Å, in which the most prominent absorption feature is the Mg-I/Mg-b triplet (MgT). We measure the line-of-sight velocity of each star by cross-correlating its spectrum against co-added Hectochelle spectra of radial velocity standards. We also measure a composite magnesium index, $\Sigma$Mg, from the weighted sum of pseudo-equivalent widths for each individual line of the MgT (see Walker et al. 2007).

We follow SG07 in modelling the velocity error as the sum of random and systematic components: the error in the $i^{th}$ measurement is $\sigma_i = \sqrt{\sigma^2_{\rm ran,i} + \sigma^2_{\rm sys}}$. We determine the random errors, which correlate with S/N, using a bootstrap method. For the $i^{th}$ spectrum, we generate 1000 artificial spectra by adding randomly generated Poisson deviates to the counts at each pixel. After measuring the velocity for each artificial spectrum, we equate $\sigma^2_{\rm ran,i}$ with the variance of the artificial distribution. We

*OBSERVATIONS REPORTED HERE WERE OBTAINED AT THE MMT OBSERVATORY, A FACILITY OPERATED JOINTLY BY THE UNIVERSITY OF ARIZONA AND THE SMITHSONIAN INSTITUTION.

Electronic address: walker@ast.cam.ac.uk
[1] Institute of Astronomy, University of Cambridge, UK
[2] Department of Astronomy, University of Michigan, Ann Arbor
[3] Steward Observatory, The University of Arizona, Tucson, AZ

then use repeat Hectochelle observations of 98 stars (including 11 Leo V targets) to determine the systematic error common to all measurements. The value $\sigma_{\rm sys} = 0.35$ km s$^{-1}$ best satisfies our requirement that the distribution of $(V_1 - V_2)(\sigma^2_{\rm ran,1} + \sigma^2_{\rm ran,2} + 2\sigma^2_{\rm sys})^{-1/2}$ resemble a Gaussian with unit variance. By the same procedure, we estimate the systematic error of ΣMg to be 0.091 Å. Among likely Leo V members in our sample, the mean (median) velocity error is ±2.2 km s$^{-1}$ (±1.6 km s$^{-1}$).

Table 1 presents spectroscopic data for the 11 stars that have velocity in the range $162 < V/$ (km s$^{-1}$) $< 180$, around the systemic mean reported in Paper I. The complete data set is available as an electronic table.

Leo V's low luminosity implies that most of the stars overlapping its red giant branch are late-type dwarfs in the Milky Way foreground. To the eye, the Leo V population appears in Figure 1 as a clump with narrow velocity distribution at small radius and weak ΣMg. We quantify this separation using an expectation-maximization (EM) algorithm similar to those devised for determining membership in open clusters (e.g., Sanders 1971). Our algorithm (see Walker et al. 2009 for details) iteratively evaluates $V$ and ΣMg distributions and assigns to each star a probability, $\hat{P}_M$, of belonging to the member population. The algorithm converges after identifying seven stars as likely members of Leo V.

Three stars (L5-31, L5-60 and L5-116 in Table 1) that would have been considered members after applying a conventional $3\sigma$ velocity threshold are identified as foreground ($\hat{P}_M < 0.01$), based on strong ΣMg and large distance from the Leo V center. Two other stars (L5-52 and L5-57) at large radius ($R \sim 13'$) are likely members ($\hat{P}_M = 0.7 \pm 0.3$ and $\hat{P}_M = 0.8 \pm 0.3$, respectively, where the reported error is derived from Monte Carlo tests in which we repeat the EM algorithm after resampling $V$ and ΣMg from the sets of artificial spectra) based on their weak ΣMg values, which fall almost exactly on the mean value for Leo V. We find no members between $3' < R < 13'$. Given Leo V's measured half-light radius of $r_{\rm h} = 0.8' \pm 0.1'$ (Paper I), the presence of two members beyond this gap is unexpected unless Leo V's morphology is highly distorted (see Section 5).

## 3. VELOCITY DISPERSION AND DYNAMICAL MASS

Assuming Leo V has a Gaussian velocity distribution with mean $\langle V \rangle$ and variance $\sigma^2_{V_0}$, the data have 2D likelihood $L(\langle V \rangle, \sigma_{V_0}) \propto \prod_{i=1}^{N} [(\sigma^2_{V_0} + \sigma^2_{V_i})^{-1/2} \exp[(V_i - \langle V \rangle)^2/(2[\sigma^2_{V_i} + \sigma^2_{V_0}])]^{M_i}$, where exponent $M = 1$ for member stars and $M = 0$ for contaminants. The values $M_i$ are unknown, but we can use the membership probabilities as weights in evaluating the expected log-likelihood given by[4]

$$E(\ln L) = -\frac{1}{2}\sum_{i=1}^{N} \hat{P}_{M_i} \ln(\sigma^2_{V_0} + \sigma^2_{V_i}) - \frac{1}{2}\sum_{i=1}^{N} \hat{P}_{M_i} \left[ \frac{(V_i - \langle V \rangle)^2}{\sigma^2_{V_0} + \sigma^2_{V_i}} \right] + \text{const.} \quad (1)$$

[4] Our results are insensitive to our implicit assumption that the velocity error distributions are Gaussian. If we instead use the exact error distributions we obtain from the sets of artificial spectra, we obtain the same constraints on the velocity dispersion.

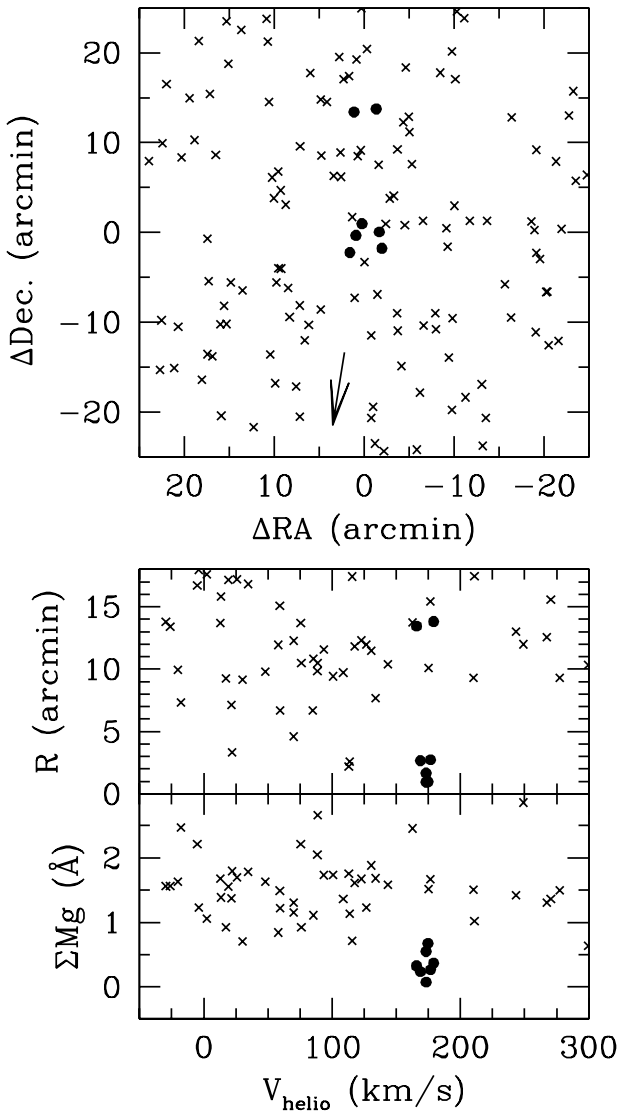


FIG. 1.— MMT/Hectochelle specotroscopic data for red giant candidates in Leo V. *Top:* Sky positions of measured stars. Solid circles (crosses) indicate likely members (nonmembers), for which the EM algorithm returns $P_M > 0.5$ ($P_M < 0.5$). An arrow points toward the Leo IV satellite, which has central coordinates $(27, -165)$. *Middle:* Projected distance from the Leo V center vs. line-of-sight velocity. *Bottom:* Magnesium index vs. velocity. The two members at large radius fall in the middle of Leo V's ΣMg distribution.

Because we are interested primarily in $\sigma^2_{V_0}$, we follow Kleyna et al. (2004) in considering the one-dimensional likelihood given by $L_{1D}(\sigma^2_{V_0}) = \int_{-\infty}^{+\infty} L(\langle V \rangle, \sigma^2_{V_0}) d\langle V \rangle$. Again treating the probabilities $\hat{P}_M$ as weights, we evaluate the 1D expected likelihood

$$E(\ln L_{1D}) = -\frac{1}{2}\ln a - \frac{1}{2}\left(c - \frac{b^2}{a}\right) - \frac{1}{2}\sum_{i=1}^{N} \hat{P}_{M_i} \ln(\sigma^2_{V_i} + \sigma^2_{V_0}) + \text{const}, \quad (2)$$

where $a = \sum_{i=1}^{N} \hat{P}_{M_i}/(\sigma^2_{V_i} + \sigma^2_{V_0})$, $b = \sum_{i=1}^{N} \hat{P}_{M_i} V_i/(\sigma^2_{V_i} + \sigma^2_{V_0})$, and $c = \sum_{i=1}^{N} \hat{P}_{M_i} V_i^2/(\sigma^2_{V_i} + \sigma^2_{V_0})$. We obtain error bounds by evaluating the area beneath the curve given by $\hat{L}_{1D} = \exp[E(\ln L_{1D})]$.

TABLE 1
Hectochelle Spectroscopy of Leo V (abridged: complete table is available in electronic version)

| Target | $\alpha_{2000}$ (hh:mm:ss) | $\delta_{2000}$ (dd:mm:ss) | $R$ (arcmin) | $r$ (mag) | $g-r$ (mag) | $V_{helio}$ (km s$^{-1}$) | $\Sigma$Mg (Å) | $P_M$ |
|---|---|---|---|---|---|---|---|---|
| L5-001 | 11:31:13.21 | +02:12:51.6 | 1.0 | 20.43 | 0.64 | $173.4 \pm 3.8$ | $0.07 \pm 0.38$ | $1.000 \pm 0.000$ |
| L5-002 | 11:31:10.59 | +02:14:09.5 | 1.0 | 19.85 | 0.78 | $174.8 \pm 0.9$ | $0.68 \pm 0.16$ | $1.000 \pm 0.000$ |
| L5-004 | 11:31:02.88 | +02:13:14.7 | 1.7 | 19.53 | 0.71 | $173.2 \pm 1.5$ | $0.55 \pm 0.16$ | $0.996 \pm 0.003$ |
| L5-007 | 11:31:01.66 | +02:11:25.2 | 2.7 | 19.67 | 0.74 | $168.8 \pm 1.6$ | $0.24 \pm 0.32$ | $0.994 \pm 0.005$ |
| L5-008 | 11:31:15.91 | +02:10:57.6 | 2.7 | 19.53 | 0.73 | $176.8 \pm 2.1$ | $0.27 \pm 0.22$ | $0.996 \pm 0.002$ |
| L5-031 | 11:31:46.64 | +02:09:10.9 | 10.1 | 20.80 | 0.70 | $175.2 \pm 1.8$ | $1.52 \pm 0.19$ | $0.000 \pm 0.000$ |
| L5-052 | 11:31:14.11 | +02:26:36.4 | 13.4 | 20.90 | 0.50 | $165.6 \pm 2.4$ | $0.39 \pm 0.25$ | $0.735 \pm 0.353$ |
| | | | | | | $166.0 \pm 2.6$ | $0.23 \pm 0.20$ | |
| L5-055 | 11:30:14.90 | +02:14:30.1 | 13.7 | 20.55 | 0.59 | $162.8 \pm 1.6$ | $2.46 \pm 0.32$ | $0.000 \pm 0.000$ |
| L5-057 | 11:31:04.15 | +02:26:56.5 | 13.8 | 21.31 | 0.42 | $179.2 \pm 3.7$ | $0.37 \pm 0.21$ | $0.788 \pm 0.304$ |
| L5-060 | 11:30:53.03 | +01:58:20.2 | 15.4 | 19.94 | 0.77 | $176.7 \pm 3.2$ | $1.67 \pm 0.52$ | $0.000 \pm 0.290$ |
| L5-116 | 11:32:22.01 | +01:56:49.3 | 24.4 | 21.00 | 1.00 | $174.6 \pm 2.0$ | $0.90 \pm 0.29$ | $0.000 \pm 0.000$ |

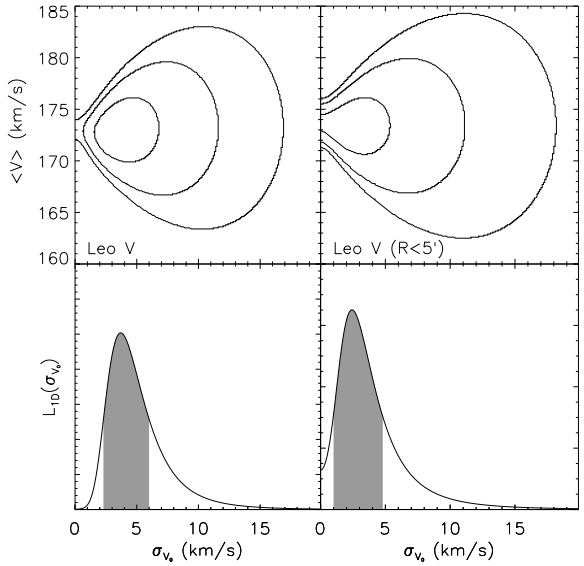


Fig. 2.— Mean velocity and velocity dispersion of Leo V, from the entire kinematic sample ($\sim 7$ members; left panels) and from stars within $5'$ of the Leo V center ($\sim 5$ members; right panels). Contours in upper panels enclose 68%, 95% and 99% of the volume underneath the likelihood surface described by Equation 1. Lower panels give the 1D likelihood of the velocity dispersion, with the shaded region marking the central 68% of the area under the curve.

Because of the bimodal distribution of $R$ among the likely Leo V members, we measure two sets of distribution parameters. Hereafter, "global" refers to the entire sample (7 members), while "central" pertains to a sample restricted to stars with $R < 5'$ (5 members).

Figure 2 (top) displays contours in the $(\langle V \rangle, \sigma_{V_0})$ plane that enclose 68%, 95%, and 99% of the volume underneath the surface given by $\hat{L} = \exp[E(\ln L)]$. While the mean velocity and global velocity dispersion are well constrained, we resolve the central velocity dispersion only marginally. This result holds also when we consider the 1D likelihood of the velocity dispersion (lower panels in Figure 2). We measure a global velocity dispersion of $\sigma_{V_0} = 3.7^{+2.3(+6.6)}_{-1.4(-2.3)}$ km s$^{-1}$ and a central velocity dispersion of $\sigma_{V_0} = 2.4^{+2.4(+7.0)}_{-1.4(-2.4)}$ km s$^{-1}$, where errors indicate 68% (95%) confidence levels. Thus at 95% confidence we rule out zero dispersion only for the global sample and cannot state conclusively that we resolve the central velocity dispersion.

Assuming the five central members are bound, we estimate the dynamical mass of Leo V using a crude "mass-follows-light" (MFL) model in which the density profile of any dark halo is proportional to that of the stellar component, and which implies total mass $M = \eta r_h \sigma^2_{V_0}$ (Illingworth 1976). For the purpose of comparing to published estimates for other satellites we adopt $\eta = 850 \mathrm{M}_\odot \mathrm{pc}^{-1} \mathrm{km}^{-1} \mathrm{s}^2$, the value corresponding to a King (1962) profile with concentration parameter characteristic of brighter dSphs (Mateo 1998). With this value and the measured central velocity dispersion we obtain $M = 3.3^{+9.1(+46)}_{-2.5(-3.3)} \times 10^5 M_\odot$ and $M_{\mathrm{MFL}}/L_V = 75^{+230(+1200)}_{-58(-74)}$. While the lower mass limit should be interpreted as consistent with a purely stellar population free of dark matter, even the upper limit gives Leo V one of the lowest dynamical masses of the SDSS satellites with measured kinematics (SG07, Martin et al. 2007; Geha et al. 2008).

## 4. METALLICITY

We estimate metallicity by comparing spectra to the library of Lee et al. (2008), based on a regularly sampled grid on which $[\alpha/\mathrm{Fe}] = 0.4$ covers a metallicity range $-4.0 <$[Fe/H]$< -0.5$, effective temperature $3500K < T_{\mathrm{eff}} < 9750$K, and surface gravity $0.0 < \log g < 5.0$. Since individual LeoV spectra at $R = 25000$ have insufficient S/N to perform a reliable spectral analysis we averaged the 5 central member spectra and, after suitable Gaussian smoothing, rebinned this average spectrum to a resolution of $R = 10000$. After continuum normalizing both data and model spectra, we compare the data directly to a suitable subset of the synthetic spectra using a masked least-squares minimization. The adopted mask isolates regions where significant absorption lines (typically with peaks $< 0.97$ of the continuum) appear in the model spectrum (Figure 3).

This free-form fit gives a well-defined solution centered on $T_{\mathrm{eff}} = 5000 \pm 250$K, [Fe/H]$= -2.0 \pm 0.3$ dex and $\log g = 2.0 \pm 1.0$. Reassuringly, if we use the relationship $\log_{10}(T_{\mathrm{eff}}) = 3.877 - 0.26(g-r)$ (Ivezić et al. 2006), the average color ($\langle g-r \rangle = 0.72$) of the five central members independently implies $\langle T_{\mathrm{eff}} \rangle = 4900$K, consistent with the temperature we derive directly from the continuum-normalized spectra. Anchoring the value of $T_{\mathrm{eff}}$ for the spectral fit tightens constraints on gravity and metallicity, giving $\log g = 2.0 \pm 0.5$ and [Fe/H]$= -2.0 \pm 0.2$ dex. The average color, magnitude, surface gravity and effective temperature are fully consistent with early K-giants at the distance of Leo V (see, e.g., Gray 2005, p. 57).

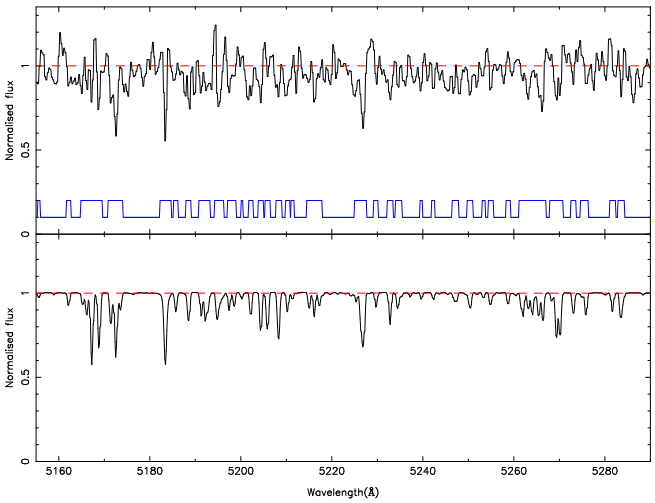


FIG. 3.— *Top:* Stacked spectrum (continuum-normalised, averaged and rebinned) for the central 5 Leo V members. *Bottom:* the best fit model spectrum; and in blue above the mask used in the minimisation.

## 5. DISCUSSION

Because we do not necessarily resolve the central velocity dispersion, we can neither place a meaningful lower limit on the dynamical mass nor state definitively that Leo V is a dark-matter-dominated dSph rather than a diffuse star cluster devoid of dark matter. In fact the data lend some support to the latter interpretation, suggesting that Leo V is an outlier with respect to two empirical scaling relations among dSphs. First, its dynamical mass-to-light ratio ($M/L_V = 75^{+233}_{-58}[M/L_V]_\odot$) likely falls short of the more extreme values ($\sim 10^{2-3}[M/L_V]_\odot$) exhibited by dSphs of similar luminosity (e.g., Figure 15 of SG07). Second, at [Fe/H]$= -2.0 \pm 0.2$ dex, Leo V is metal-rich compared to dSphs of similar luminosity, which typically have [Fe/H]$\sim -2.5$ (SG07, Kirby et al. 2008).

Despite ambiguities regarding the classification of Leo V, one conclusion is clear: the available data are inconsistent with the notion that Leo V is an equilibrium system with half-light radius $r_h = 0.8' \pm 0.1'$ ($\sim 50$ pc), the value measured from the surface brightness of its red giants (Paper I). Assuming Leo V is a uniformly sampled (c.f. Figure 1) Plummer sphere, the probability of finding at least two members, in a sample of seven, at $R \geq 10r_{\rm h}$ is $\sim 10^{-4}$. Thus our detection of two members at $R \sim 13'$ ($\sim 700$ pc) implies a distorted morphology of the sort that might arise if the two outer members belong to an unbound tidal stream. The extreme velocities of these two stars—they contribute the smallest and the largest velocities among members—further suggests that they are unbound.

Tidal interactions with the MW produce stellar streams observable in several MW satellites—for example, the Pal 5 globular cluster (Odenkirchen et al. 2003) and the Sagittarius dwarf galaxy (e.g., Majewski et al. 2003). However, Leo V, at a distance of $D \sim 180$ kpc (Paper I), will be unaffected by MW tides unless its orbit is strongly radial. If Leo V is on a radial orbit, then its journey from near the center of the MW to its present position must have taken $\sim 1$ Gyr. Assuming the two outer stars were once bound to Leo V and were stripped at the most recent pericentric passage, then they could have plausibly moved a distance of $\sim 700$ pc along the tidal tail in this time (see Equation 7 of Odenkirchen et al. 2003).

We argue in Paper I that Leos IV and V are likely companions, in which case their systemic velocities imply a nearly circular orbit that would render MW tides unimportant. In this case the two satellites might interact with each other in filamentary substructure of the sort produced in cosmological N-body simulations (e.g., Diemand et al. 2007). The fact that Leo V's two outer stars lie along the line connecting Leo IV to Leo V (Figure 1, top) provides some support for this scenario, as do the extended distributions of BHBs around both systems (Fig. 4 of Paper I).

Alternatively, Leo V may be a loosely bound star cluster losing stars to evaporation. It is not clear whether such a large cluster could form in isolation, but Leo V may have been stripped from a progenitor among the more luminous MW dSphs. The best candidate is Leo II ($D \sim 220$ kpc, $V_{\rm GSR} \sim 22$ km s$^{-1}$), which lies within $\sim 1.1^\circ$ of the orbit of the prospective Leo IV/V stream. It is also possible that a progenitor with low surface brightness lurks outside the SDSS footprint, in which case it should be detectable with data from upcoming deep-imaging surveys such as Pan-STARRS (Kaiser et al. 2002) and the Southern Sky Survey (Keller et al. 2007).

MGW acknowledges support from the STFC-funded Galaxy Formation and Evolution programme at the Institute of Astronomy, Cambridge. MM acknowledges support from NSF grants AST-0206081 0507453, and 0808043. EO acknowledges support from NSF Grants AST-0205790, 0505711, and 0807498.

## REFERENCES

Belokurov et al. 2007, ApJ, 654, 897
—. 2008, ApJ, 686, L83
Diemand, J., Kuhlen, M., & Madau, P. 2007, ApJ, 657, 262
Geha, M., Willman, B., Simon, J. D., Strigari, L. E., Kirby, E. N., Law, D. R., & Strader, J. 2008, ArXiv:0809.2781
Gray, D. F. 2005, The Observation and Analysis of Stellar Photospheres (Cambridge University Press)
Illingworth, G. 1976, ApJ, 204, 73
Ivezić et al. 2006, Memorie della Societa Astronomica Italiana, 77, 1057
Kaiser et al. 2002, in SPIE, Vol. 4836, 154–164
Keller et al. 2007, PASA, 24, 1
King, I. 1962, AJ, 67, 471
Kirby, E. N., Simon, J. D., Geha, M., Guhathakurta, P., & Frebel, A. 2008, ApJ, 685, L43
Kleyna, J. T., Wilkinson, M. I., Evans, N. W., & Gilmore, G. 2004, MNRAS, 354, L66
Koposov et al. 2008, ApJ, 686, 279
Lee et al. 2008, AJ, 136, 2050
Majewski, S. R., Skrutskie, M. F., Weinberg, M. D., & Ostheimer, J. C. 2003, ApJ, 599, 1082
Martin, N. F., Ibata, R. A., Chapman, S. C., Irwin, M., & Lewis, G. F. 2007, MNRAS, 380, 281
Mateo, M., Olszewski, E. W., & Walker, M. G. 2008, ApJ, 675, 201
Mateo, M. L. 1998, ARA&A, 36, 435
Odenkirchen et al. 2003, AJ, 126, 2385

Sanders, W. L. 1971, A&A, 14, 226
Simon, J. D., & Geha, M. 2007, ApJ, 670, 313
Walker, M. G., Mateo, M., Olszewski, E. W., Bernstein, R., Sen, B., & Woodroofe, M. 2007, ApJS, 171, 389
Walker, M. G., Mateo, M., Olszewski, E. W., Sen, B., & Woodroofe, M. 2009, AJ, 137, 3109
Willman et al. 2005, AJ, 129, 2692
York et al. 2000, AJ, 120, 1579
Zucker et al. 2006, ApJ, 650, L41